Robotica (2009) volume 27, pp. 771–778. © 2008 Cambridge University Press
doi:10.1017/S0263574708005201 Printed in the United Kingdom

Kinematics and statics analysis of a novel 4-dof 2SPS+2SPR parallel manipulator and solving its workspace

Yi Lu*, Ming Zhang, Yan Shi and JianPing Yu

Robotics Research Centre, School of Mechanical Engineering, Yanshan University Qinhuangdao, Hebei, 066004, P. R. China

(Received in Final Form: October 7, 2008. First published online: November 10, 2008)

SUMMARY

A novel 4-dof 2SPS+SPR parallel kinematic machine is proposed, and its kinematics, statics, and workspace are studied systematically. First, the geometric constrained equations are established, and the inverse displacement kinematics is analyzed. Second, the poses of active/constrained forces are determined, and the formulae for solving inverse/forward velocities are derived. Third, the formulae for solving inverse/forward accelerations are derived. Finally, a workspace is constructed and its active/constrained forces are solved. The analytic results are verified by its simulation mechanism to be consistent with the calculated ones.

KEYWORDS: Parallel manipulator; Kinematics; Statics; Workspace.

Nomenclature

B, m:	the base and the moving platform
r_i :	the active leg and its length
l_i, L_i:-	the side of m and the side of B
P, S:	the prismatic joint and the spherical joint
R_1, R_4:	the revolute joints
O, o:	the center point of B and the center point of m
$\{m\}$:	coordinate o-xyz fixed on m
$\{B\}$:	coordinate O-XYZ fixed on B
b_i, B_i:	the vertices of m and the vertices of B
$\boldsymbol{v}_r$:	the general inverse velocity
e, E:	the distances from a_i to o and from A_i to O
$\boldsymbol{\delta}_i$,:	the unit vectors of r_i
$\boldsymbol{F}$, $\boldsymbol{T}$:	the concentrated force and torque applied on m at o
$\boldsymbol{F}_{ai}$:	the active forces exerted on r_i
$\boldsymbol{F}_c$:	the constrained force
$\boldsymbol{c}_j$:	the unit vectors of $\boldsymbol{F}_{cj}$
$\mathbf{J}$, $\mathbf{H}$:	the general Jacobian matrix and Hessian matrix
x_l, x_m, x_n:	direction cosine between x and X, x and Y, x and Z
y_l, y_m, y_n:	direction cosine between y and X, y and Y, y and Z
z_l, z_m, z_n:	direction cosine between z and X, z and Y, z and Z
α, β, γ:	Euler angles of m
X_o, Y_o, Z_o:	the position components of m at o in $\{B\}$
$\boldsymbol{V}$:	the forward general velocity, $\boldsymbol{V} = [\boldsymbol{v}\ \boldsymbol{\omega}]^T$
$\boldsymbol{A}$:	the forward general acceleration, $\boldsymbol{A} = [\boldsymbol{a}\ \boldsymbol{\varepsilon}]^T$
W:	the reachable workspace
$\parallel$, $\perp$:	parallel constraint and perpendicular constraint

* Corresponding author. E-mail: luyi@ysu.edu.cn

1. Introduction

Recently, some 4-dof (degree of freedom) parallel kinematic machines (PKMs) have attracted much attention because of their relatively large workspace, simple structure, larger capability of load bearing, and easy control.[1–3] In the aspects of synthesis, kinematics, and dynamics, Carricato[3] synthesized a fully isotropic a 4-dof PKM with Schoenflies motion (three translations and one rotation). Fang and Tsai[4] synthesized some 4-dof PKMs by the screws theory. Li and Huang[5] revealed some structural characteristics of the 4-dof PKMs by constraint–synthesis. Kong and Gosselin,[6] Cornpany,[7] and Choi[8] studied various 4-dof PKMs with Schonflies motion. Alizade[9] and Gao[10] synthesized some 4-dof PKMs with parallel active limbs. Chen[11] proposed a 4-dof hybrid PKM with two translations and two rotations. Gallardo–Alvarado *et al.*[12] analyzed the kinematics and singularity of a 4-dof PKM by the screw theory. Zhang and Gosselin[13] proposed *n*-dof PKMs with a passive constraining leg. Lu and Hu[14] studied the kinematics of a 4-dof 3UPS+UPR PKM. Joshi and Tsai[15] developed a Jacobian matrix for limited-dof PKMs. Kim,[16] Merlet[17] *et al.* studied Jacobian matrix of various PKMs by adopting different approaches. Zhou *et al.*[18] studied the kinematics of some limited-dof PKMs. Lu[19,20] analyzed the kinematics and statics of some limited-dof PKMs by the CAD variation geometry. Dasgupta[21] solved the inverse dynamics by using the Newton–Euler formulation. Tsai[22] solved the inverse dynamics of a Stewart–Gough PKM by the principle of virtual work. Gallardo[23] analyzed the dynamics of PKMs by the screw theory. Using the vector analytic approach, Russo *et al.*[24] studied the static balancing of parallel robots. However, no efforts were made toward the analysis of the kinematics/statics of the 4-dof 2SPS+2SPR PKM.

Since the 2SPS+2SPR PKM includes six spherical joints which are simple in structure, large in workspace, and easy to control, this PKM has the potential applications for parallel machine tools, parallel sensors, surgical manipulators, leg or wrist of robot, tunnel borers, barbette of warship, satellite

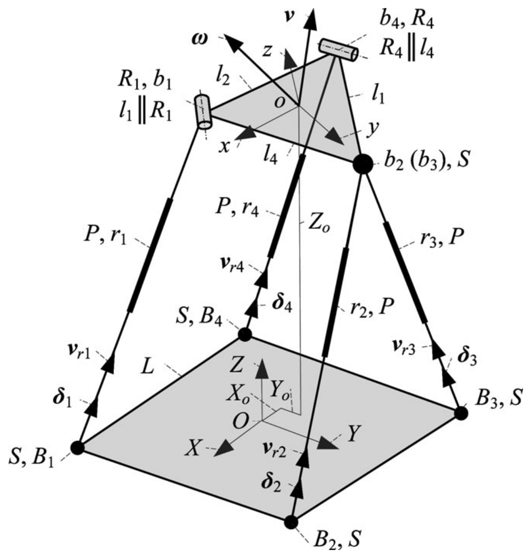

Fig. 1. The 2SPS+2SPR PKM.

surveillance platforms, and so on. For this reason, this paper focuses on the analysis of the kinematics, statics, and workspace of this PKM.

2. The 2SPS+SPR PKM and its dofs

A 2SPS+2SPR PKM (see Fig. 1a) includes a moving platform m, a fixed base B, and four active legs r_i ($i = 1$, 2, 3, 4) with linear actuator for connecting m with B.

Where m is an equilateral ternary link $\Delta b_1 b_2 b_4$ with three sides $l_1 = l_2 = l_4 = l$, four connection points b_i (b_2 coincident with b_3), and a central point o. B is a square $B_1B_2B_3B_4$ with four sides $L_i = L$, four connection points B_i, and a central point O. Let $\{m\}$ be a coordinate system o-xyz fixed on m at o, $\{B\}$ be a coordinate system O-XYZ fixed on B at O. Let $\perp$ be a parallel constraint, and $\|$ be a perpendicular constraint. Two SPS (spherical joint-prismatic joint- spherical joint) active legs connect m at b_i with B at B_i ($i = 1$, 4), and two SPR (spherical joint-prismatic joint- revolute joint) active legs connect m at b_i with B at B_i ($i = 2$, 3). Axis of revolute joint R_1 at b_1 on m is parallel with b_3b_4. Axis of revolute joint R_4 at a_4 on m is parallel with b_1b_2. Thus, the structure constraints $l_1 \perp r_1$ and $e_2 \perp r_4$ should be satisfied.

Since each of the SPS active legs r_i ($i = 1$, 3) only bears the active force along r_i, it obviously has a relative larger capacity of load bearing and is simple in structure.

In the 2SPS+2SPR PKM, the number of links is $g_0 = 10$ for one platform, four cylinders, four piston-rods, and one base; the number of joints is $g = 12$ for four prismatic joints, two revolute joints, and six spherical joints. Located dof is $M_0 = 2$ for two SPS legs rotated about their own axes. Based on a revised Kutzbach–Grübler equation,[1,2] the dof M of this PKM is calculated as

$$M = 6(g_0 - g - 1) + \sum_{i=1}^{g} m_i - M_0 = 6 \times (10 - 12 - 1) + (6 \times 1 + 6 \times 3) - 2 = 4 \qquad (1)$$

3. Analysis of Inverse Displacement

Before analyzing the kinematics and statics of the 2SPS+2SPR PKMs, the positions of the joints B_i on B and the joints b_i on m must be determined. The position vectors $\boldsymbol{b}_i{}^m$ and $\boldsymbol{b}_i$ of vertices b_i ($i = 1, 2, 3, 4$) in $\{m\}$ and $\{B\}$, and position vectors $\boldsymbol{B}_i$ of vertices B_i in $\{B\}$ can be expressed as follows:[1,2]

$$\boldsymbol{b}_i^m = \begin{bmatrix} x_{bi} \\ y_{bi} \\ z_{bi} \end{bmatrix}, \quad \boldsymbol{b}_i = \begin{bmatrix} X_{bi} \\ Y_{bi} \\ Z_{bi} \end{bmatrix}, \quad \boldsymbol{B}_i = \begin{bmatrix} X_{Bi} \\ Y_{Bi} \\ Z_{Bi} \end{bmatrix}, \quad \boldsymbol{o} = \begin{bmatrix} X_o \\ Y_o \\ Z_o \end{bmatrix},$$

$$\mathbf{R}_m^B = \begin{bmatrix} x_l & y_l & z_l \\ x_m & y_m & z_m \\ x_n & y_n & z_n \end{bmatrix}, \quad \boldsymbol{b}_i = \mathbf{R}_m^B \boldsymbol{b}_i^m + \boldsymbol{o}, \qquad (2a)$$

where (X_o, Y_o, Z_o) are the three position components of m at o in $\{B\}$; $\boldsymbol{o}$ is a vector of point o on m in $\{B\}$; $\mathbf{R}_m^B$ is a rotational transformation matrix from $\{m\}$ to $\{B\}$; $(x_l, x_m, x_n, y_l, y_m, y_n, z_l, z_m, z_n)$ in $\mathbf{R}_m^B$ are the nine orientation parameters of m, their constrained equations can be obtained from refs. [1, 2]. $\boldsymbol{b}_i^m$, $\boldsymbol{b}_i$, and $\boldsymbol{B}_i$ ($i = 1, 2, 3, 4$) can be derived from Eq. (2a) as follows:

$$\boldsymbol{b}_1^m = \frac{e}{2}\begin{bmatrix} q \\ -1 \\ 0 \end{bmatrix}, \quad \boldsymbol{b}_2^m = \boldsymbol{b}_3^m = \begin{bmatrix} 0 \\ e \\ 0 \end{bmatrix}, \quad \boldsymbol{b}_4^m = -\frac{e}{2}\begin{bmatrix} q \\ 1 \\ 0 \end{bmatrix},$$

$$\boldsymbol{B}_1 = \frac{L}{2}\begin{bmatrix} 1 \\ -1 \\ 0 \end{bmatrix}, \quad \boldsymbol{B}_2 = \frac{L}{2}\begin{bmatrix} 1 \\ 1 \\ 0 \end{bmatrix}, \quad \boldsymbol{B}_3 = \frac{L}{2}\begin{bmatrix} -1 \\ 1 \\ 0 \end{bmatrix},$$

$$\boldsymbol{B}_4 = \frac{L}{2}\begin{bmatrix} -1 \\ -1 \\ 0 \end{bmatrix}. \qquad (2b)$$

$$\boldsymbol{b}_1 = \frac{1}{2}\begin{bmatrix} qex_l - ey_l + 2X_o \\ qex_m - ey_m + 2Y_o \\ qex_n - ey_n + 2Z_o \end{bmatrix}, \quad \boldsymbol{b}_2 = \boldsymbol{b}_3 = \begin{bmatrix} ey_l + X_o \\ ey_m + Y_o \\ ey_n + Z_o \end{bmatrix},$$

$$\boldsymbol{b}_4 = \frac{1}{2}\begin{bmatrix} -qex_l - ey_l + 2X_o \\ -qex_m - ey_m + 2Y_o \\ -qex_n - ey_n + 2Z_o \end{bmatrix}, \qquad (2b)$$

where e is the distance from b_i to o, and $q = 3^{1/2}$.

Let $\boldsymbol{R}_i$ ($i = 1, 4$) be the unit vector of revolute joint R_i in $\{B\}$. They can be derived as follows:

$$\boldsymbol{R}_1 = \frac{\boldsymbol{b}_4 - \boldsymbol{b}_3}{qe} = -\frac{1}{2}\begin{bmatrix} x_l + qy_l \\ x_m + qy_m \\ x_n + qy_n \end{bmatrix},$$

$$\boldsymbol{R}_4 = \frac{\boldsymbol{b}_1 - \boldsymbol{b}_2}{qe} = \frac{1}{2}\begin{bmatrix} x_l - qy_l \\ x_m - qy_m \\ x_n - qy_n \end{bmatrix}. \qquad (2c)$$

Let α, β, γ be the three Euler angles of m, φ be one of (α, β, γ, $\gamma + 60°$, $\gamma + 30°$, and $\gamma + 45°$). Set $s_\varphi = \sin\varphi$, $c_\varphi = \cos\varphi$ and $t_\varphi = \tan\varphi$. Let the rotational transformation matrix $\mathbf{R}_m^B$ be formed by rotational order of ZYZ, namely, a rotation of α

https://doi.org/10.1017/S0263574708005201 Published online by Cambridge University Press

about Z-axis, followed by a rotation of β about Y_1-axis, and then a rotation of γ about Z_2-axis, where Y_1 is formed by Y rotating about Z by α; Z_2 is formed by Z_1 rotating about Y_1 by β. Thus, $\mathbf{R}_m^B$ can be expressed as[1]

$$\mathbf{R}_m^B = \begin{bmatrix} c_\alpha c_\beta c_\gamma - s_\alpha s_\gamma & -c_\alpha c_\beta s_\gamma - s_\alpha c_\gamma & c_\alpha s_\beta \\ s_\alpha c_\beta c_\gamma + c_\alpha s_\gamma & -s_\alpha c_\beta s_\gamma + c_\alpha c_\gamma & s_\alpha s_\beta \\ -s_\beta c_\gamma & s_\beta s_\gamma & c_\beta \end{bmatrix} \tag{2d}$$

Comparing Eq. (2a) with Eq. (2d), (x_l, x_m, x_n, y_l, y_m, y_n, z_l, z_m, z_n) can be expressed by (α, β, γ) as

$$\begin{aligned} &x_l = c_\alpha c_\beta c_\gamma - s_\alpha s_\gamma,\ x_m = s_\alpha c_\beta c_\gamma + c_\alpha s_\gamma,\\ &x_n = -s_\beta c_\gamma,\ y_l = -c_\alpha c_\beta s_\gamma - s_\alpha c_\gamma,\\ &y_m = -s_\alpha c_\beta s_\gamma + c_\alpha c_\gamma,\ y_n = s_\beta s_\gamma\\ &z_l = c_\alpha s_\beta,\ z_m = s_\alpha s_\beta,\ z_n = c_\beta. \end{aligned} \tag{2e}$$

Two constrained equations are derived from the structure constraints $l_1 \perp r_1$ and $e_2 \perp r_4$ as follows:

$$\boldsymbol{R}_1 \cdot (\boldsymbol{b}_1 - \boldsymbol{B}_1) = 0, \quad \boldsymbol{R}_4 \cdot (\boldsymbol{b}_4 - \boldsymbol{B}_4) = 0 \tag{3a}$$

From Eqs. (2c) and (3a), leads to

$$\boldsymbol{R}_1 \cdot \boldsymbol{o} = \boldsymbol{R}_1 \cdot (\boldsymbol{B}_1 - \boldsymbol{e}_1), \quad \boldsymbol{R}_4 \cdot \boldsymbol{o} = \boldsymbol{R}_4 \cdot (\boldsymbol{B}_4 - \boldsymbol{e}_4). \tag{3b}$$

From Eq. (3b), leads to

$$\begin{aligned} \begin{bmatrix} X_o \\ Y_o \end{bmatrix} &= \begin{bmatrix} X_{R1} & Y_{R1} \\ X_{R4} & Y_{R4} \end{bmatrix}^{-1} \begin{bmatrix} \boldsymbol{R}_1^T(\boldsymbol{B}_1 - \boldsymbol{e}_1) \\ \boldsymbol{R}_2^T(\boldsymbol{B}_4 - \boldsymbol{e}_4) \end{bmatrix}_{1\times 2} \\ &\quad - \begin{bmatrix} X_{R1} & Y_{R1} \\ X_{R4} & Y_{R4} \end{bmatrix}^{-1} \begin{bmatrix} Z_{R1} \\ Z_{R4} \end{bmatrix} Z_o, \end{aligned} \tag{3c}$$

where

$$\begin{aligned} \begin{bmatrix} X_{R1} & Y_{R1} \\ X_{R4} & Y_{R4} \end{bmatrix}^{-1} &= \frac{2}{qc_\beta} \begin{bmatrix} Y_{R4} & -Y_{R1} \\ -X_{R4} & X_{R1} \end{bmatrix} \\ &= \frac{2}{q} \begin{bmatrix} s_\alpha s_{\gamma+30^\circ} - \dfrac{c_\alpha c_{\gamma+30^\circ}}{c_\beta} & s_\alpha c_{\gamma+60^\circ} + \dfrac{c_\alpha s_{\gamma+60^\circ}}{c_\beta} \\ -c_\alpha s_{\gamma+30^\circ} - \dfrac{s_\alpha c_{\gamma+30^\circ}}{c_\beta} & -c_\alpha c_{\gamma+60^\circ} + \dfrac{s_\alpha s_{\gamma+60^\circ}}{c_\beta} \end{bmatrix}, \\ \boldsymbol{R}_1^T(\boldsymbol{B}_1 - \boldsymbol{e}_1) &= -\frac{L}{4}(x_l - x_m) - \frac{qL}{4}(y_l - y_m) \\ &= \frac{L}{2}[(s_\alpha - c_\alpha)c_\beta c_{\gamma+60^\circ} + (s_\alpha + c_\alpha)s_{\gamma+60^\circ}], \\ \boldsymbol{R}_4^T(\boldsymbol{B}_4 - \boldsymbol{e}_4) &= -\frac{L}{4}(x_l + x_m) + \frac{qL}{4}(y_l + y_m) \\ &= \frac{L}{2}[(c_\alpha - s_\alpha)c_{\gamma+30^\circ} - (s_\alpha + c_\alpha)c_\beta s_{\gamma+30^\circ}], \\ \begin{bmatrix} Z_{R1} \\ Z_{R4} \end{bmatrix} &= \frac{1}{2}\begin{bmatrix} -x_n - qy_n \\ x_n - qy_n \end{bmatrix} = s_\beta \begin{bmatrix} c_{\gamma+60^\circ} \\ -s_{\gamma+30^\circ} \end{bmatrix}, \\ \begin{bmatrix} X_{R1} & Y_{R1} \\ X_{R4} & Y_{R4} \end{bmatrix}^{-1} \begin{bmatrix} Z_{R1} \\ Z_{R2} \end{bmatrix} &= -t_\beta \begin{bmatrix} c_\alpha \\ s_\alpha \end{bmatrix} \end{aligned} \tag{3d}$$

Substituting all terms of Eq. (3d) into Eq. (3c), X_o and Y_o can be expressed by (α, β, γ, Z_o) as follows:

$$\begin{aligned} X_o &= Z_o c_\alpha t_\beta - \frac{2L}{q}\Big(s_\alpha c_\alpha c_\beta s_{\gamma+30^\circ} c_{\gamma+60^\circ} + 2s_\gamma c_\gamma s_{\gamma+45^\circ} c_{\gamma+45^\circ} \\ &\quad + \frac{s_\alpha c_\alpha s_{\gamma+60^\circ} c_{\gamma+30^\circ}}{c_\beta}\Big), \\ Y_o &= Z_o s_\alpha t_\beta - \frac{2L}{q}\Big(-c_\alpha^2 c_\beta s_{\gamma+30^\circ} c_{\gamma+60^\circ} + 2s_\alpha c_\alpha s_\gamma c_\gamma \\ &\quad + \frac{s_\alpha^2 s_{\gamma+60^\circ} c_{\gamma+30^\circ}}{c_\beta} + \frac{q}{4}\Big). \end{aligned} \tag{3e}$$

The extension of active legs r_i ($i = 1, 2, 3, 4$) and the unit vector δ_i of r_i can be expressed as follows:

$$r_i = |\boldsymbol{b}_i - \boldsymbol{B}_i|, \quad \boldsymbol{\delta}_i = (\boldsymbol{b}_i - \boldsymbol{B}_i)/r_i. \tag{4a}$$

Then, r_i can be expressed by (α, β, γ, Z_o) from the constrained equations of (x_l, x_m, x_n, y_l, y_m, y_n, z_l, z_m, z_n) and Eqs. (2b), (3e), and (4a) as follows:

$$\begin{aligned} r_1^2 &= X_o^2 + Y_o^2 + Z_o^2 + e^2 - L(X_o - Y_o) + L^2/2 \\ &\quad + 2e[X_o(c_\alpha c_\beta s_{\gamma+60^\circ} + s_\alpha c_{\gamma+60^\circ}) + Y_o(s_\alpha c_\beta s_{\gamma+60^\circ} \\ &\quad - c_\alpha c_{\gamma+60^\circ}) - Z_o s_\beta s_{\gamma+60^\circ}] - Le(c_\alpha - s_\alpha)c_\beta s_{\gamma+60^\circ} \\ &\quad - Le(c_\alpha + s_\alpha)c_{\gamma+60^\circ}, \\ r_2^2 &= X_o^2 + Y_o^2 + Z_o^2 + e^2 - L(X_o + Y_o) + L^2/2 \\ &\quad + 2e[-X_o(c_\alpha c_\beta s_\gamma + s_\alpha c_\gamma) - Y_o(s_\alpha c_\beta s_\gamma - c_\alpha c_\gamma) \\ &\quad + Z_o s_\beta s_\gamma] - Le(c_\alpha - s_\alpha)c_\gamma + Le(c_\alpha + s_\alpha)c_\beta s_\gamma, \\ r_3^2 &= X_o^2 + Y_o^2 + Z_o^2 + e^2 + L(X_o - Y_o) + L^2/2 \\ &\quad + 2e[-X_o(c_\alpha c_\beta s_\gamma + s_\alpha c_\gamma) - Y_o(s_\alpha c_\beta s_\gamma - c_\alpha c_\gamma) \\ &\quad + Z_o s_\beta s_\gamma] + Le(s_\alpha - c_\alpha)c_\beta s_\gamma - Le(c_\alpha + s_\alpha)c_\gamma, \\ r_4^2 &= X_o^2 + Y_o^2 + Z_o^2 + e^2 + L(X_o + Y_o) + L^2/2 \\ &\quad - 2e[X_o(c_\alpha c_\beta c_{\gamma+30^\circ} - s_\alpha s_{\gamma+30^\circ}) + Y_o(s_\alpha c_\beta c_{\gamma+30^\circ} \\ &\quad + c_\alpha s_{\gamma+30^\circ}) - Z_o s_\beta c_{\gamma+30^\circ}] - Le(c_\alpha + s_\alpha)c_\beta c_{\gamma+30^\circ} \\ &\quad - Le(c_\alpha - s_\alpha)s_{\gamma+30^\circ} \end{aligned} \tag{4b}$$

Let $\boldsymbol{\delta}_i$ ($i = 1, 2, 3, 4$) be the unit vector of r_i; $\boldsymbol{e}_i$ be the vector of line from b_i to o in $\{B\}$. They can be expended from Eqs. (2b), (4a), and (4b) as follows:

$$\delta_1 = \frac{1}{2r_1}\begin{bmatrix} qex_l - ey_l + 2X_o - L \\ qex_m - ey_m + 2X_o + L \\ qex_n - ey_n + 2Z_o \end{bmatrix},$$

$$\delta_2 = \frac{1}{2r_2}\begin{bmatrix} 2ey_l + 2X_o - L \\ 2ey_m + 2Y_o - L \\ 2ey_n + 2Z_o \end{bmatrix},$$

https://doi.org/10.1017/S0263574708005201 Published online by Cambridge University Press

$$\delta_3 = \frac{1}{2r_3}\begin{bmatrix} 2ey_l + 2X_o + L \\ 2ey_m + 2Y_o - L \\ 2ey_n + 2Z_o \end{bmatrix},$$

$$\delta_4 = \frac{1}{2r_4}\begin{bmatrix} -qex_l - ey_l + 2X_o + L \\ -qex_m - ey_m + 2Y_o + L \\ -qex_m - ey_m + 2Z_o \end{bmatrix},$$

$$\boldsymbol{e}_i = \boldsymbol{b}_i - \boldsymbol{o}, \quad \boldsymbol{e}_1 = \frac{e}{2}\begin{bmatrix} qx_l - y_l \\ qx_m - y_m \\ qx_n - y_n \end{bmatrix},$$

$$\boldsymbol{e}_2 = \boldsymbol{e}_3 = \boldsymbol{e}\begin{bmatrix} y_l \\ y_m \\ y_n \end{bmatrix}, \quad \boldsymbol{e}_4 = -\frac{e}{2}\begin{bmatrix} qx_l + y_l \\ qx_m + y_m \\ qx_n + y_n \end{bmatrix}. \quad (4c)$$

From Eqs. (2e) and (3e), $\boldsymbol{\delta}_i$ $(i = 1, 2, 3, 4)$ and $\boldsymbol{e}_i$ can be expressed by $(\alpha, \beta, \gamma, Z_o)$.

4. The Inverse/Forward Velocity and Acceleration

4.1. Inverse velocity and acceleration of the ith leg

Let $\boldsymbol{V}$ be a general forward velocity of the platform m. Let $\boldsymbol{v}$ and $\boldsymbol{\omega}$ be a linear velocity and an angular velocity of m at o, respectively. Let $\boldsymbol{v}_i$ be a velocity of m at point b_i. Let $\boldsymbol{A}$ be a general forward acceleration of m. Let $\boldsymbol{a}$ and $\boldsymbol{\varepsilon}$ be the linear acceleration and the angular acceleration of m at o, respectively. They can be expressed as follows:[1,2]

$$\boldsymbol{V} = \begin{bmatrix} \boldsymbol{v} \\ \boldsymbol{\omega} \end{bmatrix}, \quad \boldsymbol{v} = \begin{bmatrix} v_x \\ v_y \\ v_z \end{bmatrix}, \quad \boldsymbol{\omega} = \begin{bmatrix} \omega_x \\ \omega_y \\ \omega_z \end{bmatrix}, \quad \boldsymbol{A} = \begin{bmatrix} \boldsymbol{a} \\ \boldsymbol{\varepsilon} \end{bmatrix},$$

$$\boldsymbol{a} = \begin{bmatrix} a_x \\ a_y \\ a_z \end{bmatrix}, \quad \boldsymbol{\varepsilon} = \begin{bmatrix} \varepsilon_x \\ \varepsilon_y \\ \varepsilon_z \end{bmatrix}, \quad \boldsymbol{v}_i = \boldsymbol{v} + \boldsymbol{\omega} \times \boldsymbol{e}_i. \quad (5a)$$

Suppose there are two vectors $\boldsymbol{\eta}$ and $\boldsymbol{\varsigma}$, and a skew-symmetric matrix of $\boldsymbol{\eta}$. The following equations[1,14] should be satisfied

$$\boldsymbol{\eta} = \begin{bmatrix} \eta_x \\ \eta_y \\ \eta_z \end{bmatrix}, \quad \boldsymbol{\varsigma} = \begin{bmatrix} \varsigma_x \\ \varsigma_y \\ \varsigma_z \end{bmatrix}, \quad \hat{\eta} = \begin{bmatrix} 0 & -\eta_z & \eta_y \\ \eta_z & 0 & -\eta_x \\ -\eta_y & \eta_x & 0 \end{bmatrix},$$

$$\boldsymbol{\eta} \times \boldsymbol{\varsigma} = \hat{\eta}\boldsymbol{\varsigma}, \quad \hat{\eta}^T = -\hat{\eta}, \quad \hat{\eta} = \text{ one of } (\hat{\boldsymbol{\delta}}_i, \hat{\mathbf{e}}_i, \hat{\mathbf{c}}_i, \hat{\mathbf{d}}_i). \quad (5b)$$

The scalar velocities v_{ri} of the ith leg r_i along r_i have been derived from Eq. (5a) in ref. [14] as

$$v_{ri} = \left[\boldsymbol{\delta}_i^T (\boldsymbol{e}_i \times \boldsymbol{\delta}_i)^T\right]\boldsymbol{V} \quad (5c)$$

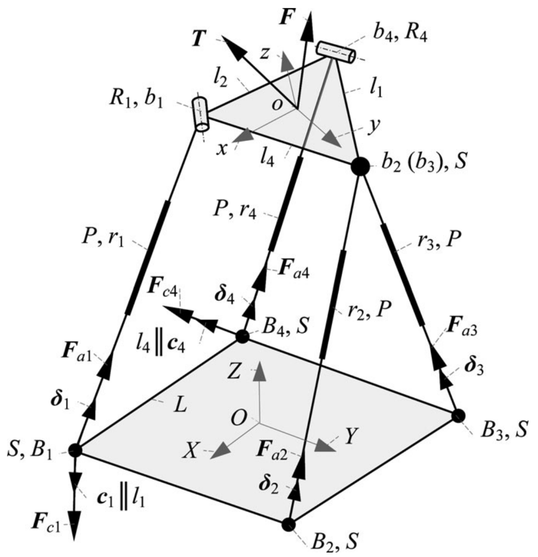

Fig. 2. Force situation of 2SPS+2SPR PKM.

The scalar accelerations a_{ri} of the ith leg r_i along r_i have been derived in ref. [14] as follows:

$$a_{ri} = \left[\boldsymbol{\delta}_i^T \ (\boldsymbol{e}_i \times \boldsymbol{\delta}_i)^T\right]\boldsymbol{A} + \boldsymbol{V}^T\mathbf{h}_i\boldsymbol{V},$$
$$\boldsymbol{h}_i = \frac{1}{r_i}\begin{bmatrix} -\hat{\delta}_i^2 & \hat{\delta}_i^2\hat{e}_i \\ -\hat{e}_i\hat{\delta}_i^2 & r_i\hat{\mathbf{e}}_i\hat{\delta}_i + \hat{\mathbf{e}}_i\hat{\delta}_i^2\hat{e}_i \end{bmatrix}_{6\times 6}. \quad (5d)$$

where $\mathbf{h}_i$ is the ith 6×6 sub-Hessian matrix.

4.2. Geometric constraints of constrained forces

The forces situation of the 2SPS+2SPR PKM is shown in Fig. 2. The whole workload can be simplified as a wrench $(\boldsymbol{F}, \boldsymbol{T})$ applied onto m at the central point o. $\boldsymbol{F}$ and $\boldsymbol{T}$ are a concentrated force and a concentrated torque applied on m at o. $(\boldsymbol{F}, \boldsymbol{T})$ includes the inertia wrench and the gravity of the platform, the inertia wrench and the gravity of the active legs which can be mapped into a part of the whole workload, the external working wrench (such as machining or operating wrench of tool and damping wrench of end effector), and the friction wrench of all the joints in PKM. $(\boldsymbol{F}, \boldsymbol{T})$ are balanced by four active forces $\boldsymbol{F}_{ai}$ $(i = 1, 2, 3, 4)$ exerted on r_i at B_i and along r_i, and two constrained forces $\boldsymbol{F}_{cj}$ $(j = 1, 4)$ exerted on r_j at B_j and parallel with axis of R_i at b_j.

Since the constrained forces $\boldsymbol{F}_{cj}$ limits the movement of the 2SPS+2SPR PKM, $\boldsymbol{F}_{ci}$ do not do any power during the movement of r_i. Thus, the two geometric constraints of $\boldsymbol{F}_{ci}$ are determined as follows:

1. Let $\boldsymbol{v}_{ri}$ be a translation velocity along prismatic joint P in SPR active leg r_j, thus $\boldsymbol{F}_{cj} \cdot \boldsymbol{v}_{rj} = 0$, i.e., $\boldsymbol{F}_{cj} \perp r_j$ must be satisfied.
2. Let $\boldsymbol{R}_j$ be a unit vector of revolute joint R_j in SPR active leg r_j, let $\rho \times \boldsymbol{F}_{cj}$ be a torque of $\boldsymbol{F}_{cj}$ about R_j. Thus, $\boldsymbol{R}_j \cdot (\rho \times \boldsymbol{F}_{cj}) = 0$ must be satisfied. That is, $\boldsymbol{F}_{cj}$ must intersect or be parallel with $\boldsymbol{R}_j$.

Since a spherical joint S can be replaced by three intersect revolute joints, an SPR-type leg can be transformed into a (3R)PR leg. From about two geometric constraints and a

https://doi.org/10.1017/S0263574708005201 Published online by Cambridge University Press

$\boldsymbol{R}_i \perp r_i$, it is inferred that the direction of vector $\boldsymbol{F}_{cj}$ exerted on r_j at B_j is the same as that of vector $\boldsymbol{R}_j$ on r_j at b_j.

4.3. General inverse/forward velocities and accelerations

Since the constrained forces $\boldsymbol{F}_{cj}$ $(j = 1, 4)$ limit movement of this PKM, $\boldsymbol{F}_{cj}$ do not do any power during the movement of this PKM. Thus, there must be

$$F_{cj}\boldsymbol{c}_j \cdot \boldsymbol{v} + (\boldsymbol{d}_j \times F_{cj}\boldsymbol{c}_j) \cdot \boldsymbol{\omega} = 0 \Rightarrow \left[\boldsymbol{c}_j^T (\boldsymbol{d}_j \times \boldsymbol{c}_j)^T\right]\boldsymbol{V} = 0, \tag{6a}$$

where $\boldsymbol{d}_j$ $(j = 1, 4)$ are the vectors of the arm from o to $\boldsymbol{F}_{cj}$. They can be solved as follows:

$$\boldsymbol{d}_1 = \boldsymbol{B}_1 - \boldsymbol{o} = \frac{1}{2}\begin{bmatrix} L - 2X_o \\ -L - 2Y_o \\ -2Z_o \end{bmatrix}, \quad \boldsymbol{d}_4 = \boldsymbol{B}_4 - \boldsymbol{o} = -\frac{1}{2}\begin{bmatrix} L + 2X_o \\ L + 2Y_o \\ 2Z_o \end{bmatrix}. \tag{6b}$$

By combining Eq. (5c) with the second equation in Eq. (6a), a general inverse velocity $\boldsymbol{v}_r$ can be derived as follows:

$$\boldsymbol{v}_r = \mathbf{J}\boldsymbol{V}, \quad \boldsymbol{v}_r = \begin{bmatrix} v_{r1} \\ v_{r2} \\ v_{r3} \\ v_{r4} \\ 0 \\ 0 \end{bmatrix}, \quad \mathbf{J} = \begin{bmatrix} \boldsymbol{\delta}_1^T & (\boldsymbol{e}_1 \times \boldsymbol{\delta}_1)^T \\ \boldsymbol{\delta}_2^T & (\boldsymbol{e}_2 \times \boldsymbol{\delta}_2)^T \\ \boldsymbol{\delta}_3^T & (\boldsymbol{e}_3 \times \boldsymbol{\delta}_3)^T \\ \boldsymbol{\delta}_4^T & (\boldsymbol{e}_4 \times \boldsymbol{\delta}_4)^T \\ \boldsymbol{c}_1^T & (\boldsymbol{d}_1 \times \boldsymbol{c}_1)^T \\ \boldsymbol{c}_4^T & (\boldsymbol{d}_4 \times \boldsymbol{c}_4)^T \end{bmatrix}_{6\times 6}, \tag{7}$$

where $\mathbf{J}$ is a 6×6 Jacobian matrix. Thus, $\mathbf{J}^{-1}$ can be solved.

Some differentiation equations are derived from Eqs. (5a), (5b), and (6b) as follows:

$$\begin{aligned} &\dot{\boldsymbol{d}}_j = -\dot{\boldsymbol{o}}^B = -\boldsymbol{v}, \quad \dot{\boldsymbol{d}}_i^T = -\boldsymbol{v}^T, \\ &\dot{\boldsymbol{c}}_1 = \boldsymbol{\omega} \times \frac{(\boldsymbol{e}_2 - \boldsymbol{e}_3)}{l} = \boldsymbol{\omega} \times \boldsymbol{c}_1, \quad \dot{\boldsymbol{c}}_4 = \boldsymbol{\omega} \times \boldsymbol{c}_4, \\ &\dot{\boldsymbol{c}}_j^T = (\boldsymbol{\omega} \times \boldsymbol{c}_j)^T = (-\hat{\mathbf{c}}_j\boldsymbol{\omega})^T = -\boldsymbol{\omega}^T\hat{\mathbf{c}}_j^T = \boldsymbol{\omega}^T\hat{\mathbf{c}}_j, \\ &(\dot{\boldsymbol{d}}_j \times \boldsymbol{c}_j + \boldsymbol{d}_j \times \dot{\boldsymbol{c}}_j)^T = [-\boldsymbol{v} \times \boldsymbol{c}_j + \boldsymbol{d}_j \times (\boldsymbol{\omega} \times \boldsymbol{c}_j)]^T \\ &= [\hat{\mathbf{c}}_j\boldsymbol{v} - \hat{\mathbf{d}}_j(\hat{\mathbf{c}}_j\boldsymbol{\omega})]^T = -\boldsymbol{v}^T\hat{\mathbf{c}}_j - \boldsymbol{\omega}^T\hat{\mathbf{c}}_j\hat{\mathbf{d}}_j. \end{aligned} \tag{8}$$

By differentiating Eq. (6a) with respect to time, from Eq. (5b) and (8), leads to

$$\begin{bmatrix} \dot{\boldsymbol{c}}_1^T & (\dot{\boldsymbol{d}}_1 \times \boldsymbol{c}_1 + \boldsymbol{d}_1 \times \dot{\boldsymbol{c}}_1)^T \\ \dot{\boldsymbol{c}}_4^T & (\dot{\boldsymbol{d}}_4 \times \boldsymbol{c}_4 + \boldsymbol{d}_4 \times \dot{\boldsymbol{c}}_4)^T \end{bmatrix}_{2\times 6} = \boldsymbol{V}^T\begin{bmatrix} \mathbf{h}_5 \\ \mathbf{h}_6 \end{bmatrix}, \quad \mathbf{h}_5 = \begin{bmatrix} \mathbf{0}_{3\times 3} & -\hat{\mathbf{c}}_1 \\ \hat{\mathbf{c}}_1 & -\hat{\mathbf{c}}_1\hat{\mathbf{d}}_1 \end{bmatrix}_{6\times 6}, \quad \mathbf{h}_6 = \begin{bmatrix} \mathbf{0}_{3\times 3} & -\hat{\mathbf{c}}_4 \\ \hat{\mathbf{c}}_4 & -\hat{\mathbf{c}}_4\hat{\mathbf{d}}_4 \end{bmatrix}_{6\times 6}. \tag{9}$$

The general inverse/forward accelerations of this PKM can be solved from Eqs. (5d) and (9) as

$$\begin{aligned} &\boldsymbol{a}_r = \mathbf{J}\boldsymbol{A} + \boldsymbol{V}^T\mathbf{H}\boldsymbol{V}, \quad \boldsymbol{A} = \mathbf{J}^{-1}(\boldsymbol{a}_r - \boldsymbol{V}^T\mathbf{H}\boldsymbol{V}) \\ &\boldsymbol{a}_r = \begin{bmatrix} a_{r1} & a_{r2} & a_{r3} & a_{r4} & 0 & 0 \end{bmatrix}^T, \\ &\mathbf{H} = \begin{bmatrix} \mathbf{h}_1 & \mathbf{h}_2 & \mathbf{h}_3 & \mathbf{h}_4 & \mathbf{h}_5 & \mathbf{h}_6 \end{bmatrix}^T, \end{aligned} \tag{10}$$

where $\mathbf{H}$ is a composite matrix with six layer. Each of the six layers includes a 6×6 sub-Hessian matrix.

5. The Statics and the Reachable Workspace

Based on the principle of virtue work[22], the power done by $(\boldsymbol{F}, \boldsymbol{T})$ must be the same as that done by active forces $\boldsymbol{F}_{ai}$ $(i = 1, 2, 3, 4)$, constrained forces $\boldsymbol{F}_{cj}$ $(j = 1, 4)$. Thus, the formulae for solving the active forces and constrained forces can be derived from Eq. (7) as below:

$$\begin{bmatrix} F_{a1} \\ F_{a2} \\ F_{a3} \\ F_{a4} \\ F_{c1} \\ F_{c4} \end{bmatrix}^T \begin{bmatrix} v_{r1} \\ v_{r2} \\ v_{r3} \\ v_{r4} \\ 0 \\ 0 \end{bmatrix}_{6\times 1} + \begin{bmatrix} \boldsymbol{F} \\ \boldsymbol{T} \end{bmatrix}^T \boldsymbol{V} = 0 \Rightarrow \begin{bmatrix} F_{a1} \\ F_{a2} \\ F_{a3} \\ F_{a4} \\ F_{c1} \\ F_{c4} \end{bmatrix} = -(\mathbf{J}^T)^{-1}\begin{bmatrix} \boldsymbol{F} \\ \boldsymbol{T} \end{bmatrix} \tag{11}$$

A reachable workspace W of the 2SPS+2SPR PKM is defined as all the positions that can be reached by the central point of the platform (see Fig. 3). When given the maximum extension $r_{\max}$ and the minimum extension $r_{\min}$ of active legs r_i $(i = 1, 2, 3, 4)$, W of the PKM can be constructed by means of its simulation mechanism[14].

For instance, set $L = 100$, l=60, $r_{\min} = 150$, $r_{\max} = 200$, $\delta r = 10$ cm, $n_1 = (r_{\max} - r_{\min})/\delta r$. W includes four upper boundary surfaces S_{ui}, four lower boundary surfaces S_{li}, and four side surfaces S_{si} $(i = 1, 2, \ldots, 4)$, see Fig. 3. Their construction processes are explained as follows:

The first upper boundary surface S_{u1} is constructed as follows:

Step 1 Set $r_3 = r_4 = r_{\max}$, $r_1 = r_{\min} + j\delta r$ $(j = 0, 1, \ldots, n_{1-}1)$.

Step 2 Set $j = 0$, vary r_2, i.e., increase r_2 by 10 at each step from $r_{\min}$ to $r_{\max}$.

Step 3 Solve the position components (X_o, Y_o, Z_o) of m in $\{B\}$ by automatically solving function of simulation mechanism in CAD software, and then insert the position components into the simulation mechanism.

Step 4 Construct a spatial curve c_0 by using the command of curve passing through XYZ.

Step 5 Repeat the steps 2 through 4 above, except that set $j = 1, 2, \ldots, n_1$, respectively. Thus, other spatial curves c_j are created.

Step 6 Construct the first upper boundary surface S_{u1} from n_1 curves c_j $(j = 0, 1, \ldots, n_{1-}1)$ by the loft command.

https://doi.org/10.1017/S0263574708005201 Published online by Cambridge University Press

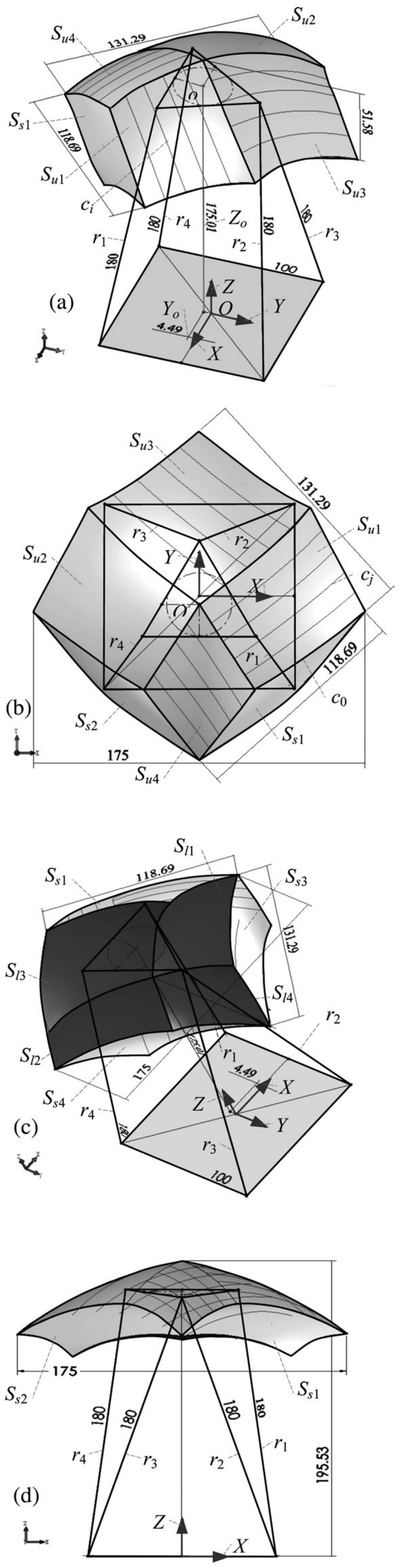

Fig. 3. Reachable workspace of the 2SPS+2SPR PKM with its simulation mechanism (a) Isometric view; (b) Tope view; (c) Upward view; (d) Front view.

Table 1. Construction processes of the subsurfaces of reachable workspace W.

S	$r_{\min}$	$r_{\max}$	$r_{\min}+j\delta r$	r varying in $r_{\min}$ $r_{\max}$	S_r
S_{u1}		r_3, r_4	r_1	r_2	S_{u2}
S_{u2}		r_1, r_2	r_3	r_4	S_{u1}
S_{u3}		r_1, r_4	r_2	r_3	
S_{u4}		r_2, r_3	r_4	r_1	
S_{s1}	r_1	r_3	r_2	r_4	S_{s2}
S_{s2}	r_4	r_2	r_3	r_1	S_{s1}
S_{s3}	r_2	r_4	r_1	r_3	S_{s4}
S_{s4}	r_3	r_1	r_4	r_2	S_{s3}
S_{l1}	r_1, r_2		r_4	r_3	S_{l2}
S_{l2}	r_3, r_4		r_2	r_1	S_{l1}
S_{l3}	r_1, r_4		r_2	r_3	
S_{l4}	r_2, r_3		r_4	r_1	

S: subsurface, S_r: reflection of S.

The construction processes of all the subsurfaces S and their reflections are summarized as shown in Table I

In fact, S_{u2}, S_{l2}, S_{s2}, and S_{s4} are the reflective surfaces of S_{u1}, S_{l1}, S_{s1}, S_{s3}, respectively. The whole workspace is symmetrical about O-YZ plane.

6. Analytic Solved Example

The workload wrench $(\boldsymbol{F}, \boldsymbol{T})$ includes the inertia wrench and the gravity of the platform, the damping wrench of platform, the equivalent inertia wrench and the gravity of the legs mapped into a part of $(\boldsymbol{F}, \boldsymbol{T})$, and the external working wrench. Therefore, when velocity, acceleration, the mass, inertia moment, mass-center, and damping coefficient of platform and legs are given, the accurate $(\boldsymbol{F}, \boldsymbol{T})$ can be solved.

Set $L = 100$ cm, $l = 60$ cm, $\boldsymbol{F} = [20\ 30\ 60]^T$ kN, $\boldsymbol{T} = [30\ 30\ 30]^T$ kN·cm. When the three Euler angles α, β, γ are increased by a velocity 0.3°/s from 0° to 6°, and given Z_o versus time (see Fig. 4a), by means of Matlab and the relevant analytic formulae Eqs. (3e), (4b), (4c), (7)–(11), the kinematics and the statics of this PKM are solved (see Fig. 4). The two position components X_o and Y_o of m are solved (see Fig. 4a). The extension, velocity, and acceleration of r_i ($i = 1$, 2, 3, 4) are solved (see Fig. 4b–d). The velocity, angular velocity, and acceleration of m are solved (see Fig. 4e–g); the active/constrained forces are solved (see Fig. 4h). These analytic solutions have been verified by the simulation solutions of simulation mechanism of this PKM in Solidwork.[19,20]

7. Conclusions

A 2SPS+2SPR parallel manipulator with two SPS active legs and two SPR active leg has four dofs, i.e., three rotations and one translation. Each of the SPS-type active legs with the linear actuator is simple in structure and has a relatively large capability of load bearing as it only bears a active force along its own axis.

The reachable workspace of this parallel manipulator is symmetric about the O-YZ plane and is quite large.

https://doi.org/10.1017/S0263574708005201 Published online by Cambridge University Press

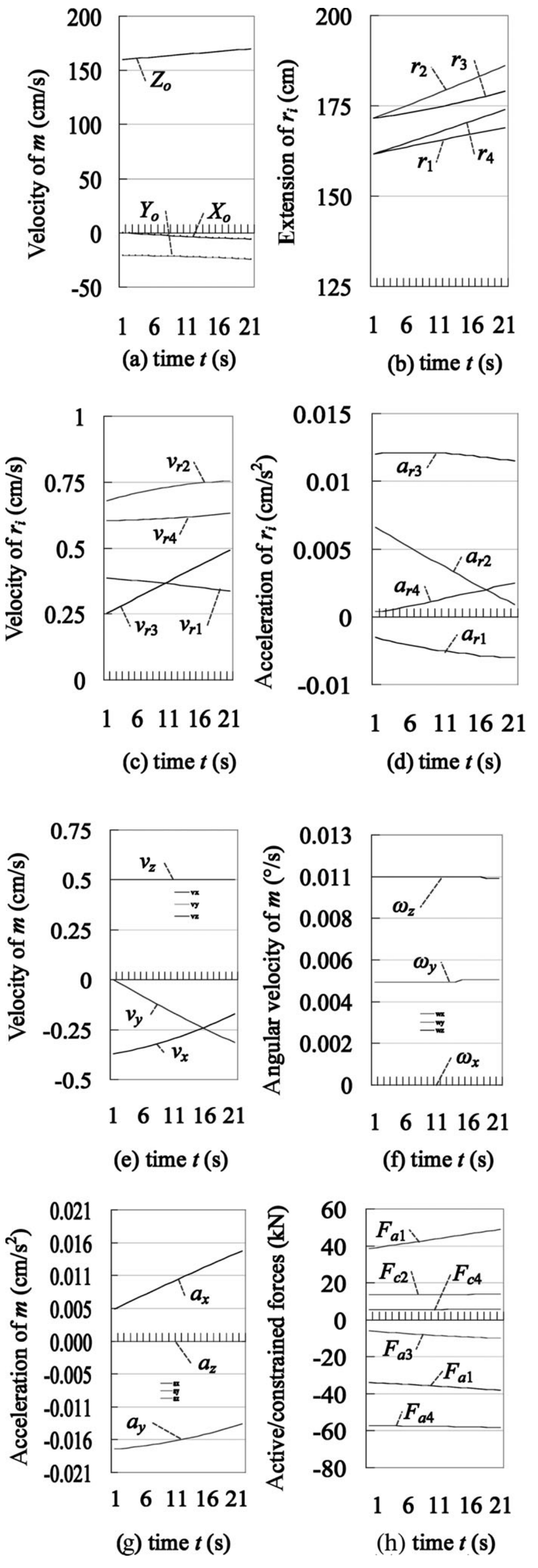

Fig. 4. Solved results of the 2SPS+2SPR PKM.

When the central point of the platform is close to the side surface of reachable workspace, the orientation parameters are increased obviously.

A 6×6 Jacobian matrix without the partial differentiation, and a $6 \times 6 \times 6$ Hessian matrix without the partial differentiation are derived, and the inverse/forward velocity and acceleration of the 2SPS+2SPR parallel manipulator are solved. The analytic results of this parallel manipulator are verified by its simulation mechanism.

The 2SPS+2SPR parallel manipulator has some potential applications for the 4-dof PMK, such as parallel machine tool, leg or wrist of robot, parallel sensor, surgical manipulator, tunnel borer, warship barbette, and satellite surveillance platform.

Acknowledgments

The authors would like to acknowledge the financial support of the Natural Sciences Foundation Council of China (NSFC) 50575198 and of Doctoral Fund from the National Education Ministry vide no. 20060216006.

References

1. S. B. Niku, *Introduction to Robotics Analysis, Systems, Applications* (Pearson Education, Publishing as Prentice Hall, and Publishing House of Electronics Industry, Beijing, 2004).
2. Z. Huang, L.-F. Kong and Y.-F. Fang, *Theory on Parallel Robotics and Control* (Machinery Industry Press, Beijing, 1997).
3. M. Carricato, "Fully isotropic four-degrees-of-freedom parallel mechanisms for Schoenflies motion," *Int. J. Rob. Res.* **24**(5), 397–414 (2005).
4. Y.-F. Fang and L. W. Tsai, "Structure synthesis of a class of 4-dof and 5-dof parallel manipulators with identical limb structures," *Int. J. Rob. Res.* **21**(9), 799–810 (2002).
5. Q. Li and Z. Huang, "Type Synthesis of 4-dof Parallel Manipulators," In *IEEE International Conference on Robotics and Automation*, Taipei (Sep. 14–19, 2003) pp. 755–760.
6. X. Kong and C. M. Gosselin, "Type synthesis of 3T1R 4-dof parallel manipulators based on screw theory," *IEEE Trans. Rob. Automat.* **20**(2), 181–190 (2004).
7. O. Company, F. Marquet and F. Pierrot, "A new high speed 4-dof parallel robot. synthesis and modeling issues," *IEEE Trans. Rob. Automat.* **19**(3), 411–420 (2003).
8. H.-B. Choi, O. Company, F. Pierrot, A. Konno, T. Shibukawa, and M. Uchiyama, "Design and control of a novel 4-dofs parallel robot H4," In *IEEE International Conference on Robotics and Automation*, Taipei, (Sep. 14–19,2003) pp. 1185–1190.
9. R. I. Alizade and C. Bayram, "Structural synthesis of parallel manipulators," *Mech. Mach. Theory* **39**(8), 857–870 (2004).
10. F. Gao, W.-M. Li, X.-C. Zhao, Z.-L. Jin and H. Zhao, "New kinematic structures for 2-, 3-, 4-, and 5-DOF parallel manipulator designs," *Mech. Mach. Theory* **37**(11), 1395–1411 (2002).
11. W.-J. Chen, "A novel 4-dof parallel manipulator and its kinematic modeling," In *IEEE International Conference on Robotics and Automation* , Seoul (May 23–25, 2001) pp. 3350–3355.
12. J. Gallardo-Alvarado, J. M. Rico-Martinez and G. Alici, "Kinematics and singularity analysis of a 4-dof parallel manipulator using screw theory," *Mech. Mach. Theory* **41**, 1048–1061 (2006).
13. D. Zhang and C. M. Gosselin, "Kinetostatic modeling of N-DOF parallel mechanisms with a passive constraining leg and prismatic actuators," *ASME J. Mech. Des.* **123**(3), 375–384 (2001).
14. Y. Lu and B. Hu, "Analyzing kinematics and solving active/constrained forces of a 3SPU+UPR parallel manipulator," *Mach. Mech. Theory* **42**(10), 1298–1313 (2007).
15. S. A. Joshi, and L. W. Tsai, "Jacobian analysis of limited-DOF parallel manipulators," *J. Mech. Des., Trans. ASME* **124**(2), 254–258 (2002).

https://doi.org/10.1017/S0263574708005201 Published online by Cambridge University Press

16. S.-G. Kim and J. Ryu, "New dimensionally homogeneous Jacobian matrix formulation by three end-effector points for optimal design of parallel manipulators," *IEEE Trans. Rob. Automat.* **19**(4), 731–737 (2003).
17. J. P. Merlet, "Jacobian, manipulability, condition number, and accuracy of parallel robots," *ASME J. Mech. Des.* **128**(1), 199–206 (2006).
18. K. Zhou, J.-S. Zhao, Z.-Y. Tan and D.-Z. Mao, "The kinematics study of a class of spatial parallel mechanism with fewer degrees of freedom," *Int. J. Adv. Manuf. Tech.* **25**(9–10), 972–978 (2005).
19. Y. Lu, "Using CAD variation geometry for solving velocity and acceleration of parallel manipulators with 3–5 linear driving limbs," *ASME J. Mech. Des.* **128**(4), 738–746 (2006).
20. Y. Lu, "Using virtual work theory and CAD functionalities for solving driving force and driven force of spatial parallel manipulators," *Mach. Mech. Theory* **42**(10), 839–858 (2007).
21. B. Dasgupta and T. S. Mruthyunjaya, "A Newton-Euler formulation for the inverse dynamics of the Stewart platform manipulator," *Mech. Mach. Theory* **33**(8), 1135–1152 (1998).
22. L. W. Tsai, "Solving the inverse dynamics of a Stewart-Gough manipulator by the principle of virtual work," *ASME J. Mech. Des.* **122**(1), 3–9 (2000).
23. J. Gallardo, J. M. Rico, A. Frisoli, D. Checcacci and M. Bergamasco, "Dynamics of parallel manipulators by means of screw theory," *Mech. Mach. Theory* **38**(11), 1113–1131 (2003).
24. R. Andrea, S. Rosario and X. Fengfeng, "Static balancing of parallel robots Mechanism and Machine Theory," *Mech. Mach. Theory* **40**(2), 191–202 (2005).